Variation in vertebrae shape across small-bodied newts reveals functional and developmental constraints acting upon the trunk region

Scholtes, S.J.; Arntzen, J.W.; Ajduković, M.; Ivanović, A.

Received: 21 March 2021 | Revised: 31 October 2021 | Accepted: 1 November 2021

DOI: 10.1111/joa.13591

Journal of Anatomy ANATOMICAL SOCIETY WILEY

ORIGINAL PAPER

Variation in vertebrae shape across small-bodied newts reveals functional and developmental constraints acting upon the trunk region

Stefan J. Scholtes[1] | Jan W. Arntzen[1] | Maja Ajduković[2] | Ana Ivanović[3]

[1]Naturalis Biodiversity Center, Leiden, The Netherlands

[2]Department of Evolutionary Biology, Institute for Biological Research "Siniša Stanković", National Institute of Republic of Serbia, University of Belgrade, Belgrade, Serbia

[3]Faculty of Biology, University of Belgrade, Belgrade, Serbia

Correspondence
Stefan J. Scholtes, Naturalis Biodiversity Center, Leiden, The Netherlands.
Email: sjscholtes@gmail.com

Funding information
Serbian Ministry of Education, Science and Technological Development of the Republic of Serbia, Grant/Award Number: 451-03-68/2020-14/200178 and 451-03-9/2021-14/200007

Abstract

The salamander vertebral column is largely undifferentiated with a series of more or less uniform rib-bearing presacral vertebrae traditionally designated as the trunk region. We explored regionalization of the salamander trunk in seven species and two subspecies of the salamander genus *Lissotriton* by the combination of microcomputed tomography scanning and geometric morphometrics. The detailed information on trunk vertebral shape was subjected to a multidimensional cluster analysis and a phenotypic trajectory analysis. With these complementary approaches, we observed a clear morphological regionalization. Clustering analysis showed that the anterior trunk vertebrae (T1 and T2) have distinct morphologies that are shared by all taxa, whereas the subsequent, more posterior vertebrae show significant disparity between species. The phenotypic trajectory analysis revealed that all taxa share a common pattern and amount of shape change along the trunk region. Altogether, our results support the hypothesis of a conserved anterior-posterior developmental patterning which can be associated with different functional demands, reflecting (sub)species' and, possibly, regional ecological divergences within species.

KEYWORDS
geometric morphometrics, high-dimensional clustering analysis, *Lissotriton*, micro computed tomography, phenotypic trajectory analysis, regionalization, trunk vertebrae

1 | INTRODUCTION

The vertebral column forms the central axis of the vertebrate body and has a crucial role in body support and locomotion. It is composed of a number of repetitive, serially homologous skeletal elements—the vertebrae. The homeobox (*Hox*) genes are known to be directly involved in somite and vertebrae formation and play a key role in the attainment of vertebral identity (Krumlauf, 1994; Mallo et al., 2010; Woltering, 2012). It has been proposed that different vertebral morphologies are governed by unique combinations of *Hox* genes expressed in the somites (Kessel & Gruss, 1991; Wellik, 2007) with the corollary that few *Hox* genes expression boundaries can be used as markers for regional differentiation of the axial skeleton (Böhmer et al., 2015; Burke et al., 1995; Narita & Kuratani, 2005). For example, the cervico-thoracic transition in amniotes is determined by *Hox*-5 and *Hox*-6 genes and the formation of the lumbo-sacral boundary is under control of the *Hox*-10 and *Hox*-11 genes (Wellik & Capecchi, 2003). Recent morphometric studies have provided new insight into presacral vertebral regionalization in amniotes (Head & Polly, 2015; Jones et al., 2018, 2020; Terray et al., 2020). A subtle morphological gradient along the anterior–posterior axis was found in stem members of amniotes and in squamates, including snakes and limbless lizards (Head & Polly, 2015). As these authors remarked regionalization may not be restricted to amniotes. Salamanders,

being the only group of lower vertebrates with a generalized tetrapod body plan, are an appropriate model to look into this hypothesis.

So far data on developmental pattering of vertebral column in amphibians are scarce (Woltering et al., 2009; Worthington & Wake, 1972). The presacral vertebral column of salamanders is regarded as poorly differentiated (Duellman & Trueb, 1994; Mivart, 1870) and evolutionary changes reported are mostly numerical (Arntzen et al., 2015; Bonett & Blair, 2017). The conservancy of presacral region has been attributed to conflicting demands that are imposed by a biphasic life cycle with different modes of locomotion, namely swimming and walking (Bonett & Blair, 2017).

The salamander's presacral vertebral column is composed of the atlas, a single vertebra that articulates with the skull, and a series of rib-bearing vertebrae, traditionally designated as the trunk region (Figure 1a). Some differentiation within the trunk region was described by Funk (1827). In his detailed account on the anatomy of the fire salamander, he recognized the thoracic region (composed of the first, second, and third trunk vertebrae) and associated this morphological section with sternum support. Worthington and Wake (1972) found in several salamander species that vertebrae relative proportions (i.e., length) may vary among anterior and posterior trunk vertebrae and alluded to a functional significance. Finally, a quantitative analysis of morphological variation of the presacral vertebral region in the salamander genus *Ambystoma* revealed a subtle regional differentiation (Jones et al., 2018, 2020). The regionalization in *Ambystoma* corresponds to the regionalization found in amniotes with three regions: the cervical region consisting of the first three trunk vertebrae and related to brachial plexus, followed by seven anterior dorsal and five posterior dorsal vertebrae, corresponding to the regions with "long" and "short" ribs (Jones et al., 2018).

To investigate regionalization of trunk vertebrae in salamanders, we choose a group of small-bodied newts of the Eurasian genus *Lissotriton* that are well represented in museum collections. These newts have overall similar habitat preferences, but show substantial genetic and geographic differentiation among and sometimes within species (Babik et al., 2005; Frost, 2021; Wielstra et al., 2018). The number of trunk vertebrae in the genus is 12, exceptionally 13 (Arntzen et al., 2015). This conservancy in the number of vertebrae allows for a comparative analysis of morphological variation and differentiation because the serial homology of vertebrae is a reasonable assumption. We applied microcomputed tomography scanning (micro-CT scanning) and 3D geometric morphometrics techniques to describe the shape of each trunk vertebrae, and to analyze the differentiation of vertebrae along the trunk region of individuals belonging to same taxon. Finally, we compared the differentiation of trunk vertebrae between taxa in a phylogenetic context, to find out whether the regionalization is phylogenetically conserved. If, for example, the regionalization of the trunk is common to all taxa, then vertebrae morphology is probably under strong developmental and functional constraints.

2 | MATERIALS AND METHODS

We studied 118 adult male newts of seven species and two subspecies of the genus *Lissotriton* with sample sizes of 7–25 specimens per taxon. For species names, taxonomic authority, localities, sample

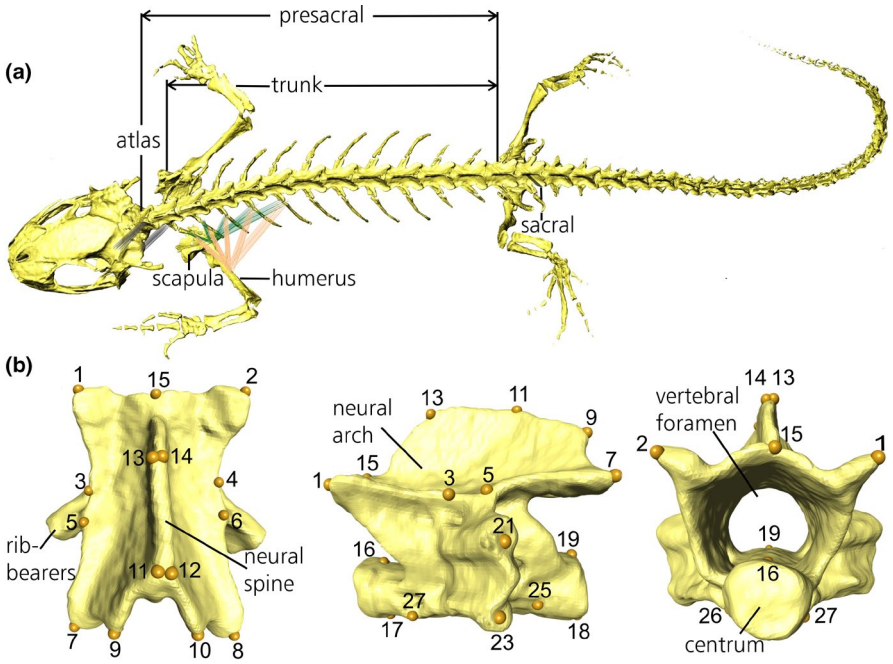

FIGURE 1 Three-dimensional surface model of a *Lissotriton* skeleton with (a) a schematic presentation of the musculature that connects the skull (gray), the pectoral girdle (dark green), and the forelimb (orange) to the proximal part of trunk region (T1–T5) and (b) the second trunk vertebra (T2) in detail. Brief anatomical descriptions of the 27 landmarks are given in Table S2

sizes, and preservation status (ethanol preserved specimens or glycerine preserved skeletons) see Table S1. For geographical distribution of the (sub-)species of the genus *Lissotriton* (after Arntzen et al., 2009, 2009; Ianella et al., 2017; Wielstra et al., 2018) and sample localities see Figure S1. The phylogenetic relationships of the studied taxa are described by Pabijan et al. (2017) and Rancilhac et al. (2020).

Data gathering was performed with the SkyScan 1172 micro-CT scanner (Bruker Corporation) under the following parameters: 26.33 μM resolution, 32 kV, 0.5 μM aluminium filter, 0.7 degrees rotation steps, 175 ms exposure time, 180 degrees object scanning, and a manual flat field correction set at 35 kV. The reconstructed images were supplied as input for three-dimensional visualization with Avizo 9.5 software (FEI, Thermo Fisher Scientific).

For each specimen we constructed a three-dimensional surface model of the entire trunk region (Figure 1a). Trunk vertebrae (thus, all presacral vertebrae excluding the atlas) were numbered in anteroposterior order, from T1 to T12 (T1–T13 in the studied populations of *Lissotriton v. vulgaris*). Twenty-seven landmarks were applied to each trunk vertebra with Avizo's landmark module. A visual representation of the landmark configuration is provided in Figure 1b and brief anatomical descriptions of the landmarks are presented in Table S2.

The following procedures were executed in the R Statistical Environment version 3.5.1 (Core Team, 2018). Digitized landmark configurations were imported with the package "Arothron" (Profico et al., 2021). Shape variables for each trunk vertebra were extracted through a Generalized Procrustes Analysis (GPA) that accounts for object symmetry (Klingenberg et al., 2002), using the package "geomorph" (Adams et al., 2021). To determine the clusters of morphologically similar vertebrae, we used the "HDclassif" software package (Bergé et al., 2012). The entire set of 1441 trunk vertebrae (with all vertebrae pooled, irrespective of species or vertebral identity) was used as input for the clustering analysis. To avoid possible recognition of false clusters (see Rohlf, 2021), we used an unsupervized pattern recognition analyses under model evaluation with the Bayesian information criterion. This identified the "AjBQD" model as the best choice.

The clustering analysis assigns each vertebra in the dataset to a defined cluster (vertebral morphotype) and the identifications where subsequently summarized according to proportionality of identified morphotypes along the antero–posterior axis (T1–T12 or T13) and corresponding species, (Table S3). A principal component analysis (PCA) was performed to visualize the relative position of the identified morphotypes in morphospace and to explore variation in vertebrae shape between morphotypes.

For a comparative analysis, we applied a phenotypic trajectory analysis across taxa (PTA) (Adams & Collyer, 2009; Collyer & Adams, 2013). This analysis allows for pairwise statistical assessment of: (1) trajectory size, that is the amount of species-specific shape change along the trunk, (2) trajectory shape, that is the pattern of shape change between vertebrae along the trunk region, and (3) trajectory direction, that is the general orientation of shape changes in multivariate shape space. The PTA requires standardization of the number of trunk vertebrae used. All species in the dataset had 12 trunk vertebrae, except for *L. v. vulgaris*, which has 13. Visual inspection of the proximity of trunk vertebral means of *L. v. vulgaris* in morphospace showed that vertebrae T7 and T8 are almost entirely overlapping and therefore deemed very similar in shape. A multivariate analysis of variance (MANOVA) found no difference in shape of T7 and T8 ($p = 0.995$). Vertebra T7 was subsequently removed from the analysis to facilitate the comparative analysis. The PCA, PTA, and MANOVA were carried out with the software package "geomorph" (Adams et al., 2021).

3 | RESULTS

The clustering procedure allocated the altogether 1441 trunk vertebrae from nine *Lissotriton* (sub-) species into eight groups, which we designated "morphotypes" A to H. The relative positioning of these groups in shape space is presented in Figure 2. The first principal component axis describes the variation in vertebra length and the size and height of the vertebral foramen and accounts for 48.1% of the total variance in the data. The second principal component axis describes the variation in neural spine height and accounts for 10.6% of the observed variation. Along PC1 morphotype A is characterized by short and high vertebrae with a large vertebral foramen. On the opposite end of this axis sits morphotype H with long and low vertebrae that have a small vertebral foramen. Along PC2 types A and H with low neural spines are most differentiated from morphotype E vertebrae that have high and rounded neural spines. The C- and D-morphotypes have intermediate shapes, with medium high neural spines that are rounded in the C-type and thick and square shaped in the D-type. The D-type morphotype is separated along PC3 that describes 6.3% of the total variance in vertebrae shape. The B-morphotype is intermediate to types A and E and the F- and G-morphotypes are intermediate to types E and H. The G- and H-morphotypes are similar in overall shape, but are distinguished by the relative positioning of the rib-bearers that are more posteriorly pointed in the H- than in the G-type.

Across all taxa, the first vertebra (T1) has the A-morphotype, and the second vertebra (T2) has the B-morphotype (Figure 3). The last trunk vertebra has the H-type, except for *L. graecus* and two out of three of the *L. helveticus* populations. The D-morphotype is only found in *L. boscai* (with a single exception, see Table S3). In *L. helveticus*, the discriminative power of the clustering analysis was low, apparently because the three studied populations have different morphologies. In the north of France, the E-type dominates (population Marcillé la Ville), in the south of France (population Montignac sur Vézere) the F-type is most frequent along the T5-T11 range, and in Portugal (population Areinho) the C-type is most frequent. The F-morphotype is dominant in *L. graecus* and *L. kosswigi* over the T3-T10 or T3-T12 range and is also found in the middle section (T5 and T6) of *L. v. meridionalis*. Within the *L. montandoni* – *L. vulgaris* species group – the G-morphotype prevails. The preponderance of the F-type morphology appears a derived feature of the *L. graecus* – *L. kosswigi* clade, as well as the elongation from 12 to 13 vertebrae in *L. v. vulgaris* (Figure 3). *Lissotriton vulgaris* shows a well-differentiated trunk

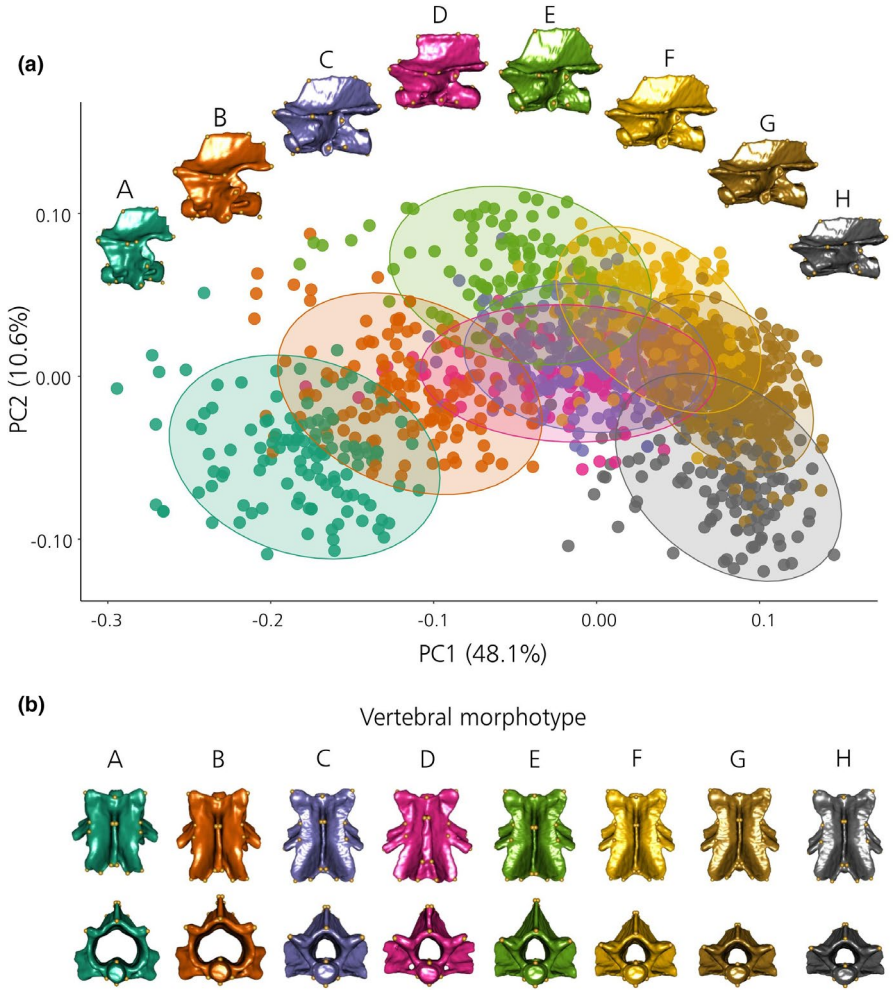

FIGURE 2 Principal component analysis (PCA) and vertebrae morphotypes: (a) Phenotypic clustering of 1441 vertebrae from nine *Lissotriton* species and subspecies in eight morphotypes (A–H) expressed over the first (PC1) and second axes (PC2). The phenotypic clustering is highlighted by 95% confidence ellipses. Three-dimensional surface models of the mean shape of each morphotype (in lateral view) are presented adjacent to the corresponding cluster. (b) Morphotypes mean shapes in dorsal (top series) and anterior view (bottom series)

region, characterized by C-type morphologies in the T3-T5 section, G-type morphologies in the T5-T11 section (except the aforementioned F-type in *L. v. meridionalis*), and H-type morphologies for the last one or last two trunk vertebrae.

The PTA showed that trajectory size (magnitude of shape changes along the trunk region) and shape (pattern of shape changes along the trunk region) are largely similar between species, subspecies, and populations ($p > 0.05$ in all pairwise comparisons, Table S4a,b). The path directions (general orientation of anterior-posterior shape change in the multivariate shape space) were all significantly different ($p < 0.01$), except for *L. v. meridionalis* and *L. kosswigi* ($p > 0.05$, Table S4c). All phenotypic trajectories exhibit the same horse-shoe shape, but differ in their position over the bivariate plot (Figure 4, Figure S2). At the apex of the "horse shoe," morphological change switches abruptly from the first to the second PC-axis.

In comparison with the identified morphotypes derived from the clustering analysis, the aberrantly shaped E-morphotype, mainly represented in the Marcillé la Ville population of *L. helveticus*, is differentiated in the second principal component of the PCA and PTA. The third principal component captured the aberrant D-morphotype represented in *L. boscai*. Differentiations of the D- and E-morphotypes found in the clustering analysis are prominently visible in PTA when comparing the second and third principal components (Figure S2 and S2_3D).

4 | DISCUSSION

We analyzed morphological variation of the trunk vertebrae in small-bodied newts (genus *Lissotriton*) by applying two complementary statistical approaches. With either method (multidimensional cluster analysis and PTA), we detected a marked regionalization of the trunk region. The shapes of the first and second trunk vertebrae are the most conserved (the A and B morphotypes), whereas the posterior vertebrae are more variable, with taxon- and even population-specific morphologies (Figure 3). Notwithstanding the observed morphological

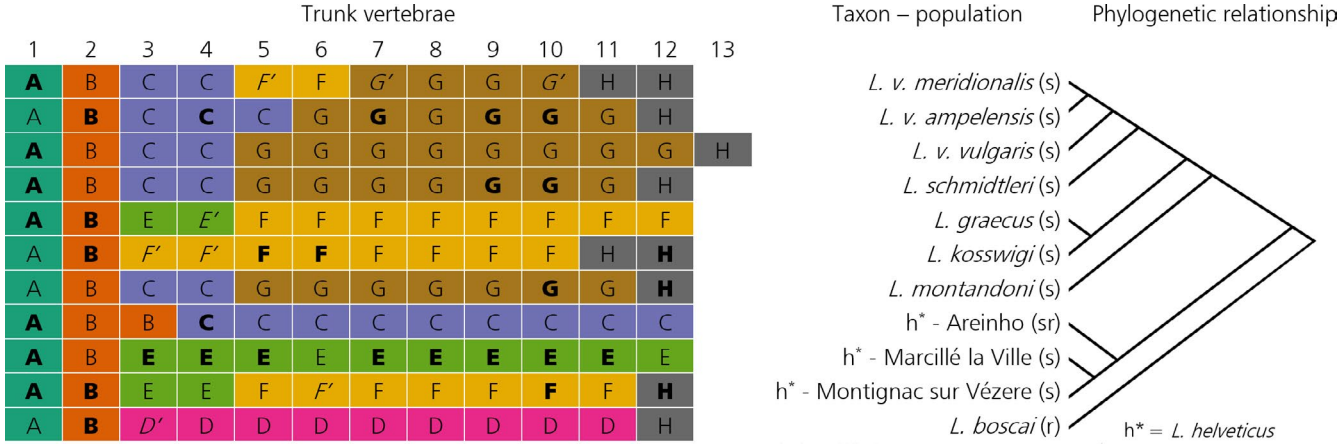

FIGURE 3 Summary of the distribution of the morphotypes (A–H) along the trunk in nine (sub-)species and three populations of the genus *Lissotriton* along with documented habitat preferences ("r" stands for running water and "s" stands for stagnant water; details see text). The phylogenetic tree is a composite of Pabijan et al. (2017) for the recent nodes and Rancilhac et al. (2020) for the deeper nodes. Cell color codes are as in Figure 2. The typeface used represents the observed morphotype frequency (f) as follows: f = 1.00 is in bold type, 0.60<f<1.00 is in normal type, and 0.33<f<0.60 is in italics marked with an apostrophe ('). The constituent data are in Table S3

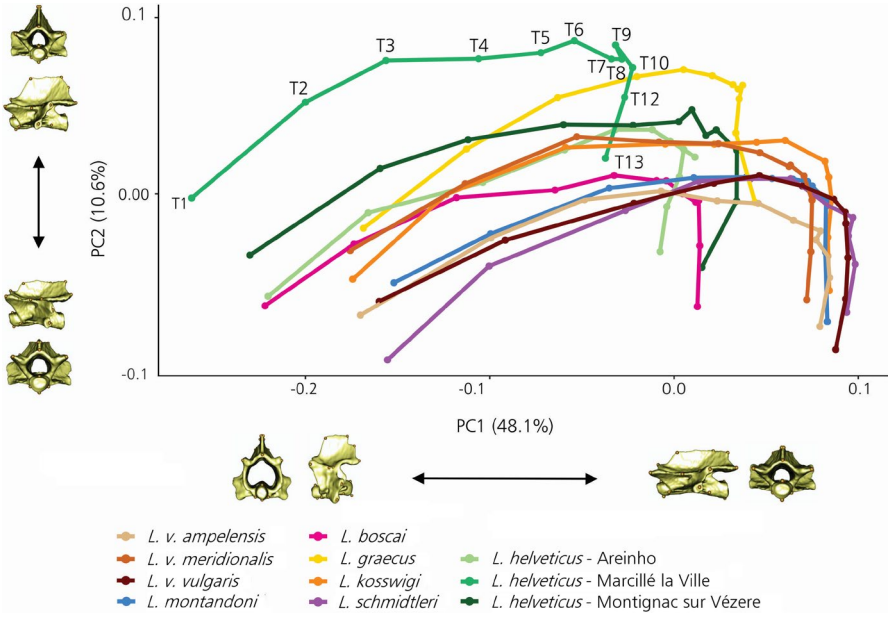

FIGURE 4 Phenotypic trajectories of shape changes along the trunk of the newt genus *Lissotriton*, expressed over the first (PC1) and second principal component axes (PC2). Trajectories were calculated for nine (sub-)species. The three populations of the *L. helveticus* were analyzed separately. Taxa are coded by colors as shown in the legend. Connected dots represent the mean vertebrae (T) shape from T1 to T12, as is highlighted for *L. helveticus* from Marcillé la Ville, France. Three-dimensional surface models visualize the corresponding shape changes

regionalization, the trajectories of shape change are similar among taxa (Figure 4), from which we conclude that the regionalization of the presacral vertebrae is largely conserved.

4.1 | Developmental basis of trunk regionalization

The observed, weak regionalization of trunk region in *Lissotriton* supports the hypothesis that regionalization is conserved across the tetrapods (Head & Polly, 2015; Jones et al., 2018) but subtly expressed. Unfortunately, the data on *Hox* gene expressions in amphibians are mostly related to the development of limb skeleton and not the vertebral column (Mannaerta et al., 2006; Totok et al., 1998). If, however, the generalized pattern of *Hox* expression (paralog groups 4–10) operates across the tetrapods (Head & Polly, 2015; Wellik, 2007), then the observed regionalization within the trunk region is presumably the result of common development governed by these genes and subsequently altered by different functional and ecological demands.

4.2 | Trunk regionalization and functional demands

The regionalization of vertebral column reflects specific locomotor adaptations and behavior. In salamanders, locomotion is achieved by lateral bending and undulation of the spine, which is a part of swimming as well as (terrestrial) stepping (Azizi, 2005; Karakasiliotis et al., 2012). The proximal part of the trunk region is, however, also involved in foraging, head digging, the bending of the spine, and it supports the pectoral girdle. To reveal possible functional (locomotor) constraints acting upon trunk region, we explored the relationship between vertebrae and skeletal muscles involved in locomotion and body support. The most detailed description of the musculoskeletal system is by Francis (1934) for *Salamandra salamandra* and is here taken as a *pars pro toto* for salamandrid salamanders, including *Lissotriton*.

The proximal trunk vertebrae (T1-T5) have different functional demands compared with the subsequent trunk vertebrae (Figure 1a). The muscles involved in head movement are the *m. rectus capitis posterior* and the *m. intertransversarius capitis inferior* that arise from the atlas and the transverse process of T1, respectively. The latter muscle induces the lateral flexion of the spine and turns the head from side to side. The differentiation and conservancy of T1 (the A morphotype shared by all individuals regardless to the species or population of origin) can be related to its physical connection with the cranium, in particular its specific function in movement of the head. The specific morphology of T2 (the B morphotype) is also shared by all individuals (vertebra with a large vertebral foramen, but more elongated compared with the A morphotype). The straight part of the *m. thoraciscapularis* (*m. serratus magnus*) arises from T1 and T2 and inserts on the suprascapular and acts as a depressor of the scapula. The anatomical position (with a direct connection to T1) and slightly different function most likely underlie the conservancy of T2. The oblique part of *m. thoraciscapularis* arises from T2 to T5 and retracts the scapula. The *m. dorso humeralis* that also arises from the anterior vertebrae is involved in locomotion as a retractor of the humerus (Figure 1a). Despite a similar function, the shapes of the vertebrae T3, T4, and T5 are more variable. In the majority of (sub-)species the T3, T4, and T5 belong to two different morphotypes. However, in populations of *L. boscai* and *L. helveticus*, the vertebrae in the T3-T5 section have a same morphotype as remaining trunk vertebrae (Figure 3). The described variation suggests that different species or population-specific ecological preferences and locomotor requirements may alter the shape of these vertebrae.

The remaining dorsal musculature is uniform, completely segmented, subdivided by myosepta that arise from the posterior edge of the neural spine of each trunk vertebrae and innervated by spinal nerves. The fibres of the *m. dorsalis trunci* connect the subsequent vertebrae from the dorsal side. The most internal part of the ventral musculature also connects the subsequent vertebrae, while the rectus and the oblique portion of the ventral musculature extend from the pelvic girdle to the sternum or the pectoral girdle, with the main role in flexing the vertebral column. The muscles of the pelvic girdle and the hind limbs are interconnecting these skeletal elements and attach on the post sacral vertebrae. Accordingly, the trunk vertebrae are not directly functionally connected with the pelvis and hind limbs. The uniformity in muscle arrangement between T6 and the end of the trunk region (T12 or T13), and the similarity in function (bending and flexing the spine) coincide with the observed uniform shape of the posterior trunk vertebrae. Most of the species considered here exhibit only one or two vertebral types in this range, namely types F and H, or types G and H. The H morphotype characterizes the last (one or two) trunk vertebrae that articulate with the sacral vertebra. The observed differentiation of the trunk vertebrae corresponds to their specific anatomical position and functional demands and may be related to ecological and behavioral differences associated with body support and locomotion (see below).

4.3 | Ecology and evolutionary changes in *Lissotriton* vertebrae morphology

The hypothetical morphological series A-B-E-F-G-H (so without morphotypes C and D see Figure 2) describes a gradual anteroposterior elongation of the vertebrae along with a decrease of neural spine height (Figure 4). This series is (be it incompletely) represented by all studies taxa, except for *L. boscai* that has the aberrant D-type over the T3-T11 range, and *L. helveticus* that shows geographical variation. *Lissotriton boscai* is a species that frequently inhabits small streams (Caetano & Leclair, 1999) and the exceptional morphology of its vertebrae with thick, square neural spines and with two parallel ridges for the attachment of dorsal trunk muscles may be related to these particular functional demands. Morphotype C is found over the length of the trunk (T4-T12) in *L. helveticus* from Areinho, Portugal. This species prefers breeding in stagnant water bodies like small ponds, road ditches, and water tanks, but can also be found in slow flowing, temporal streams, especially toward the southern parts of it range (Galán, 1999; Galán & Fernández, 1993). This observation lends support to the hypothesis of an association between the types of vertebrae morphologies and habitat preferences. A phylogeographical component may also come into play, because the Areinho population represent a distinct, western Iberian lineage of *L. helveticus* (Recuero & García-París, 2011). On the other hand, both French populations also appear morphologically differentiated with a markedly increased neural spine height (morphotype E) in the northern population versus the more common F-type in the south, yet presumably they share the regular *Lissotriton* aquatic habitat of stagnant water and belong to the same phylogeographical lineage. The shape of the mid-trunk vertebrae is largely clade-specific: the three *L. vulgaris* subspecies and the phylogenetically closely related *L. schmidtleri* (Figure 3) share the same (A-B-C-G-H) axial patterning, be it that *L. v. meridionalis* additionally shows the F-type vertebrae (A-B-C-F-G-H). The sister species *L. graecus* and *L. kosswigi* share the same A-B-F phenotypical series. This configuration may be interpreted as a synapomorphy, given that *L. montandoni* shares the A-B-C-G-H configuration with the *L. vulgaris* group (Figure 3).

4.4 | Conclusions

The novel, high-dimensional clustering approach provided a detailed insight into morphological variation and differentiation in vertebrae shape along the trunk and in the divergences in vertebrae shape among taxa. It also assisted to define the boundaries between sub-regions, which is an important step toward defining vertebrae homology in salamander species with different and highly variable number of trunk vertebrae. However, differentiation and regionalization of trunk vertebrae in *Lissotriton* species is not the same as described for *Ambystoma* (Jones et al., 2018). The differences may reflect the deep evolutionary divergence of the *Ambystoma* and *Lissotriton* lineages (Dubois et al., 2021), but may also be affected by different methodological approaches. The clustering analysis that we used discriminates vertebrae by their shape without taking the position of the vertebra in the vertebral column into account. Conversely, the likelihood-based segmented regression approach (Jones et al., 2018) considers the vertebral column to be a series of morphological gradients and takes positional information into account. We propose that both approaches have their merits and may fruitfully be applied together to increase our understanding on the regionalization and development of the vertebral column.

ACKNOWLEDGMENTS

The authors thank collection manager Esther Dondorp and micro-CT specialist Rob Langelaan from Naturalis Biodiversity Centre, Tijana Vučić from the University of Belgrade for assistance and advice and two anonymous reviewers for their helpful comments and advice. S.J.S. thanks the Van Hall Larenstein University of Applied Sciences for the opportunity to be involved in this research through an internship. The authors have no conflicts of interest to declare.

AUTHORS CONTRIBUTIONS

S.J.S., J.W.A., and A.I. conceived and designed the study and analyzed the data. All authors contributed to the writing and revising of drafts of the paper, prepared figures, and tables and approved the final version.

DATA AVAILABILITY STATEMENT

The data that support the findings of this study are openly available in figshare at https://doi.org/10.6084/m9.figshare.14254406.

ORCID

Stefan J. Scholtes https://orcid.org/0000-0001-9320-4296
Maja Ajduković https://orcid.org/0000-0001-9115-6622
Ana Ivanović https://orcid.org/0000-0002-6247-8849

REFERENCES

Adams, D.C. & Collyer, M.L. (2009) A general framework for the analysis of phenotypic trajectories in evolutionary studies. *Evolution*, 63, 1143–1154. https://doi.org/10.1111/j.1558-5646.2009.00649.x.

Adams, D.C., Collyer, M.L., Kaliontzopoulou, A. & Baken, E. (2021) Geomorph: Software for geometric morphometric analyses. R package version 3.3.2. https://cran.r-project.org/package=geomorph

Arntzen, J.W., Beebee, T., Jehle, R., Denoël, M., Schmidt, B. & Bosch, J. et al. (2009) Lissotriton helveticus. The IUCN Red List of Threatened Species 2009: e.T59475A11948264. https://doi.org/10.2305/IUCN.UK.2009.RLTS.T59475A11948264.en

Arntzen, J.W., Beja, P., Jehle, R., Bosch, J., Tejedo, M. & Lizana, M. (2009) *Lissotriton boscai*. The IUCN Red List of Threatened Species 2009. e.T59473A11947331. https://doi.org/https://doi.org/10.2305/iucn.uk.2009.rlts.t59473a11947331.en

Arntzen, J.W., Beukema, W., Galis, F. & Ivanović, A. (2015) Vertebral number is highly evolvable in salamanders and newts (family Salamandridae) and variably associated with climatic parameters. *Contribution to Zoology*, 84, 87–116. https://doi.org/10.1163/18759866-08402001.

Azizi, E. (2005) *Biomechanics of salamander locomotion*. Amherst: University of Massachusetts.

Babik, W., Branicki, W., Crnobrnja-isailović, J., Cogalniceănu, D., Sas, I., Olgun, K. et al. (2005) Phylogeography of two European newt species—discordance between mtDNA and morphology. *Molecular Ecology*, 14, 2475–2491. https://doi.org/10.1111/j.1365-294X.2005.02605.x.

Bergé, L., Bouveyron, C. & Girard, S. (2012) HDclassif: an R package for model-based clustering and discriminant analysis of high-dimensional data. *Journal of Statistical Software*, 46, 1–29. https://doi.org/10.18637/jss.v046.i06.

Böhmer, C., Rauhut, O.W.M. & Wörheide, G. (2015) Correlation between Hox code and vertebral morphology in archosaurs. *Proceedings of the Royal Society B: Biological Sciences*, 282, 20150077. https://doi.org/10.1098/rspb.2015.0077.

Bonett, R.M. & Blair, A.L. (2017) Evidence for complex life cycle constraints on salamander body form diversification. *Proceedings of the National Academy of Sciences*, 114, 9936–9941. https://doi.org/10.1073/pnas.1703877114.

Burke, A.C., Nelson, C.E., Morgan, B.A. & Tabin, C. (1995) Hox genes and the evolution of vertebrate axial morphology. *Development*, 121, 333–346. https://doi.org/10.1242/dev.121.2.333.

Caetano, M.H. & Leclair, R. (1999) Comparative phenology and demography of *Triturus boscai* from Portugal. *Journal of Herpetology*, 33, 192–202. https://doi.org/10.2307/1565714.

Collyer, M.L. & Adams, D.C. (2013) Phenotypic trajectory analysis: comparison of shape change patterns in evolution and ecology. *Hystrix*, 24, 75–83. https://doi.org/10.4404/hystrix-24.1-6298.

Core Team, R (2018) *R: A language and environment for statistical computing*. Vienna, Austria: R Foundation for Statistical Computing https://www.R-project.org/.

Dubois, A., Ohler, A. & Pyron, R.A. (2021) New concepts and methods for phylogenetic taxonomy and nomenclature in zoology, exemplified by a new ranked cladonomy of recent amphibians (Lissamphibia). *Megataxa*, 5, 1–738 https://doi.org/10.11646/megataxa.5.1.1

Duellman, W.E. & Trueb, L. (1994) *Biology of amphibians*. Maryland: Johns Hopkins University Press.

Francis, E.B.T. (1934) *The anatomy of the salamander*. Oxford: Clarendon Press.

Frost, D.R. (2021) *Lissotriton Bell, 1839 | Amphibian Species of the World: An Online Reference*. Version 6.1. New York: American Museum of Natural History https://amphibiansoftheworld.amnh.org/Amphibia/Caudata/Salamandridae/Pleurodelinae/Lissotriton.

Funk, A.F. (1827) De Salamandrae terrestris vita: evolutione, formatione tractatus. Berline: sumbitus Dunckeri et Humblotii.

Galán, P. (1999) *Conservación de la Herpetofauna Gallega. Situación actual de los Anfibios y Reptiles de Galicia*. A Coruña: Universidade da Coruña.

Galán, P. & Fernández, G. (1993) Anfibios e Réptiles de Galicia. Vigo: Ed. Xerais.

Head, J.J. & Polly, P.D. (2015) Evolution of the snake body form reveals homoplasy in amniote Hox gene function. *Nature*, 520, 86–89. https://doi.org/10.1038/nature14042.

Iannella, M., Cerasoli, F. & Biondi, M. (2017) Unraveling climate influences on the distribution of the parapatric newts *Lissotriton vulgaris meridionalis* and *L. italicus*. *Frontiers in Zoology*, 14, 55. https://doi.org/10.1186/s12983-017-0239-4.

Jones, K.E., Angielczyk, K.D., Polly, P.D., Head, J.J., Fernandez, V., Lungmus, J.K. et al. (2018) Fossils reveal the complex evolutionary history of the mammalian regionalized spine. *Science*, 361, 1249–1252. https://doi.org/10.1126/science.aar3126.

Jones, K.E., Gonzalez, S., Angielczyk, K.D. & Pierce, S.E. (2020) Regionalization of the axial skeleton predates functional adaptation in the forerunners of mammals. *Nature Ecology & Evolution*, 4, 470–478. https://doi.org/10.1038/s41559-020-1094-9.

Karakasiliotis, K., Schilling, N., Cabelguen, J.M. & Ijspeert, A.J. (2012) Where are we in understanding salamander locomotion: biological and robotic perspectives on kinematics. *Biological Cybernetics*, 107, 529–544. https://doi.org/10.1007/s00422-012-0540-4.

Kessel, M. & Gruss, P. (1991) Homeotic transformations of murine vertebrae and concomitant alteration of Hox codes induced by retinoic acid. *Cell*, 67, 89–104. https://doi.org/10.1016/0092-8674(91)90574-i.

Klingenberg, C.P., Barluenga, M. & Meyer, A. (2002) Shape analysis of symmetric structures: quantifying variation among individuals and asymmetry. *Evolution*, 56, 1909–1920. https://doi.org/10.1111/j.0014-3820.2002.tb00117.x.

Krumlauf, R. (1994) Hox genes in vertebrate development. *Cell*, 78, 191–201. https://doi.org/10.1016/0092-8674(94)90290-9.

Mallo, M., Wellik, D.M. & Deschamps, J. (2010) Hox genes and regional patterning of the vertebrate body plan. *Developmental Biology*, 344, 7–15. https://doi.org/10.1016/j.ydbio.2010.04.024.

Mannaerta, A., Roelantsa, K., Bossuyta, F. & Leyns, L. (2006) A PCR survey for posterior Hox genes in amphibians. *Molecular Phylogenetics and Evolution*, 38, 449–458. https://doi.org/10.1016/j.ympev.2005.08.012.

Mivart, G. (1870) On the axial skeleton of the Urodela. *Proceedings of the Zoological Society of London*, 1870, 260–278.

Narita, Y. & Kuratani, S. (2005) Evolution of the vertebral formulae in mammals: a perspective on developmental constraints. *Journal of Experimental Zoology*, 304, 91–106. https://doi.org/10.1002/jez.b.21029.

Pabijan, M., Zieliński, P., Dudek, K., Stuglik, M. & Babik, W. (2017) Isolation and gene flow in a speciation continuum in newts. *Molecular Phylogenetics and Evolution*, 116, 1–12. https://doi.org/10.1016/j.ympev.2017.08.003.

Profico, A., Buzi, C., Castiglione, S., Melchionna, M., Piras, P., Veneziano, A. et al. (2021) Arothron: an R package for geometric morphometric methods and virtual anthropology applications. *American Journal of Physical Anthropology*, 176, 1–8. https://doi.org/10.1002/ajpa.24340.

Rancilhac, L., Irisarri, I., Angelini, C., Arntzen, J.W., Babik, W., Bossuyt, F. et al. (2020) Phylotranscriptomic evidence for pervasive ancient hybridization among Old World salamanders. *Molecular Phylogenetics and Evolution*, 155, 106967. https://doi.org/10.1016/j.ympev.2020.106967.

Recuero, E. & García-París, M. (2011) Evolutionary history of *Lissotriton helveticus*: multilocus assessment of ancestral vs. recent colonization of the Iberian Peninsula. *Molecular Phylogenetics and Evolution*, 60, 170–182. https://doi.org/10.1016/j.ympev.2011.04.006.

Rohlf, F.J. (2021) Why clusters and other patterns can seem to be found in analyses of high-dimensional data. *Evolutionary Biology*, 48, 1–16. https://doi.org/10.1007/s11692-020-09518-6.

Terray, L., Plateau, O., Abourachid, A., Böhmer, C., Delapré, A., de la Bernardie, X. et al. (2020) Modularity of the neck in birds (Aves). *Evolutionary Biology*, 47, 97–110. https://doi.org/10.1007/s11692-020-09495-w.

Totok, A.M., Gardiner, D.M., Shubin, N.H. & Bryant, S.V. (1998) Expression of HoxD genes in developing and regenerating axolotl limbs. *Developmental Biology*, 200, 225–233. https://doi.org/10.1006/dbio.1998.8956.

Wellik, D.M. (2007) Hox patterning of the vertebrate axial skeleton. *Developmental Dynamics*, 236, 2454–2463. https://doi.org/10.1002/dvdy.21286.

Wellik, D.M. & Capecchi, M.R. (2003) Hox10 and Hox11 genes are required to globally pattern the mammalian skeleton. *Science*, 301, 363–367. https://doi.org/10.1126/science.1085672.

Wielstra, B., Canestrelli, D., Cvijanović, M., Denoël, M., Fijarczyk, A., Jablonski, D. et al. (2018) The distributions of the six species constituting the smooth newt species complex (*Lissotriton vulgaris* sensu lato and *L. montandoni*) – an addition to the New Atlas of Amphibians and Reptiles of Europe. *Amphibia-Reptilia*, 39, 252–259. https://doi.org/10.1163/15685381-17000128.

Woltering, J.M. (2012) From lizard to snake; behind the evolution of an extreme body plan. *Current Genomics*, 13, 289–299. https://doi.org/10.2174/138920212800793302.

Woltering, J.M., Vonk, F.J., Müller, H., Bardine, N., Tuduce, I.L., de Bakker, M.A.G. et al. (2009) Axial patterning in snakes and caecilians: evidence for an alternative interpretation of the Hox code. *Developmental Biology*, 332, 82–89. https://doi.org/10.1016/j.ydbio.2009.04.031.

Worthington, R.D. & Wake, B.D. (1972) Patterns of regional variation in the vertebral column of terrestrial salamanders. *Journal of Morphology*, 137, 257–277. https://doi.org/10.1002/jmor.1051370302.

SUPPORTING INFORMATION

Additional supporting information may be found in the online version of the article at the publisher's website.

How to cite this article: Scholtes, S.J., Arntzen, J.W., Ajduković, M. & Ivanović, A. (2022) Variation in vertebrae shape across small-bodied newts reveals functional and developmental constraints acting upon the trunk region. *Journal of Anatomy*, 240, 639–646. Available from: https://doi.org/10.1111/joa.13591